Power Conditioning and Control Unit for the French Cesium Contact Ion Thruster

A. COSTES,* C. LANDRAULT,† AND M. BRIOT†
Laboratoire d'Automatique et d'Analyse des Systèmes du C.N.R.S., Toulouse, France

This paper summarizes the studies and results obtained by the "Electric Propulsion" team of the L.A.A.S. du C.N.R.S. in the domain of the preindustrialization of the French cesium contact ion thruster. The three complement topics described are the theoretical study (both static and dynamic) of the thruster which is considered as a multivariable system, the application of the results so obtained to the definition of the beam current control loop and the definition of the power conditioning and control unit. For each of the three topics, the theoretical and experimental aspects are described and the main results commented upon.

Nomenclature

A, A_i, A_p, A_v = mathematical model gain
A_c = universal constant (1.2 10^6 amp m^2)
A_f = emitting area of the neutralizer filament
A_i = emitting area of the ionizer
a = ionizer pore mean diameter
d = cesium atom mean free path
D = beam-neutralizer distance
e = electron charge
F = thrust vector amplitude
I = beam current
i = neutralizer emitted current
J = saturation beam density
k = Boltzmann's constant
K_i = integration constant
K_p = proportionality constant
l = ionizer mean pore length
L = feed line length
m_a = cesium atom mass
m_i = cesium ion mass
η = ionization efficiency
p = Laplace transform operator
p_a = vaporizer downstream pressure
p_i = ionizer upstream pressure
p_m = pipe mean pressure
Q = flow rate through the feed line
R = feed-line radius
T_i = ionizer temperature
T_m = mean temperature in the pipe
T_n = neutralizer minimum temperature
T_v = vaporizer temperature
U = positive high voltage
V = neutralizer biasing voltage
α = transmission coefficient
Δ_p = pressure loss
δ = cesium atom protection sphere
δ_p = ionizer pore density
ε_0 = permitivity of free space
ϕ_0 = ionization work function
$\tau_r, \tau_{i2}, \tau_{i3}$ = time constants

I. Introduction

OUR studies are integrated in the French study program[1] defined by the "Centre National d'Etudes Spatiales." The first part concerns the implementation of the thruster static and dynamic mathematical models. The study of sensibility to parameter variations carried out at this level, together with the knowledge of the global mathematical model and the actual thruster operation enables the definition of the different regulation loops required for an imperturbed operation around the nominal operating point. The second part is devoted to the definition of the power conditioning and control unit and the interfaces with the thruster. The third part gives the main electrical characteristics of the power supplies and the regulation loops as well as the specific performances obtained. The fourth and last part indicates the results of the tests which have been conducted on a monobutton-type cesium contact ion thruster.

II. Mathematical Model of a Cesium Contact Ion Thruster Regulation Loop Definition

Static Mathematical Model

Thrust vector amplitude

In order to determine the expression relating the thrust vector amplitude to the different control variables, we have established the various relationships existing between the thruster parameters from the vaporizer to the neutralizer (Fig. 1).[2-4]

a) Pressure downstream of the vaporizer:

$$p_a = 5.65\ 10^8 \exp(-8522/T_v)$$

b) Beam density: The ion flux from the downstream face of the ionizer can be limited by two phenomena: space charge and ionizer saturation. This second phenomenon which corresponds to the nominal operating mode takes place when the total accelerating voltage is sufficiently high to extract all the ions that are available due to the pressure upstream of the ionizer. The beam density thus presents an upper limit that is a function of the thruster characteristics

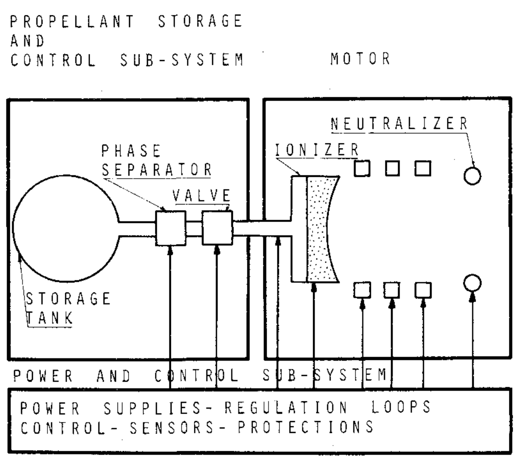

Fig. 1 Schematic diagram showing the principal elements of a contact ion propulsion system.

Presented as Paper 73-1102 at the AIAA 10th Electric Propulsion Conference, Lake Tahoe, Nev., October 31–November 2, 1973; submitted December 11, 1973; revision received May 7, 1974.
Index categories: Electric and Advanced Space Propulsion; Spacecraft Propulsion Systems Integration.
* Professor, Automatic Control.
† Research Scientists.

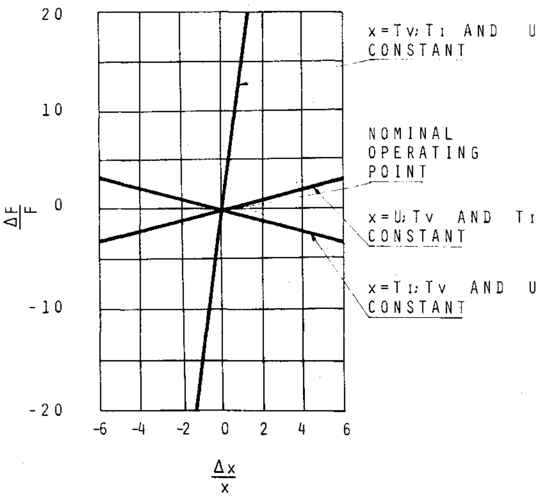

Fig. 2 Relative variations of the thrust vector amplitude.

$$J = \frac{e\alpha\eta p_i}{2k\pi T_i m_a}$$

Its computation requires the knowledge of η, p_i, and α.

1) *Determination of η:* By experiment it is known that for an ionizer temperature greater than the critical temperature, the ionization efficiency η is approximately unity.

2) *Determination of p_i:* The pressure p_i upstream of the ionizer is given by

$$p_i = 5.65 \times 10^8 \exp(-8522/T_v) - \Delta p$$

where Δp denotes the pressure loss in the feed line. According to the flow mechanism of the cesium vapor, it is given by the following expressions

laminar flow $\left(\frac{R}{d} \geq 40\right)$ $$\Delta p = \frac{5LQ}{\delta^2 R^4 p_m}\left(\frac{k^3 m_a T_m^{\ 3}}{\pi^3}\right)^{1/2}$$

molecular flow $\left(\frac{R}{d} \leq 1.5\right)$ $$\Delta p = \frac{3LQ}{4R^3}\left(\frac{k m_a T_m}{2\pi}\right)^{1/2}$$

3) *Determination of α:* The transmission coefficient α depends on the width of the ionizer pores. For large pores whose mean width is greater than 10 μm (which corresponds to an essentially molecular flow) we have

$$\alpha = \frac{\pi^2 a^3 \delta p}{1}$$

For small pores (mean width between 1 μm and 10 μm) the calculation of the various flow rates (migration flux, neutral flow from the pore inlet, neutral flow from the pore internal wall, neutral flow from evaporation) shows that the migration flow is dominant compared to the molecular flow and to the flow originating at the pore wall surface.

c) *Minimal temperature of the neutralizer filament:* The minimal operating temperature T_n of the neutralizer filament, is deduced from the Richardson-Dushman equation which gives the value of the current delivered by the neutralizer filament

$$i = A_c \frac{T_n}{A_f} \exp(-e\phi_0/kT_n)$$

d) *Neutralizer biasing voltage:* The voltage between the beam and the neutralizer filament is given by the expression

$$V = \left\{\frac{9}{4}\frac{I \cdot D^2}{\varepsilon_0 A_f}\left(\frac{m_i}{2e}\right)^{1/2}\right\}^{2/3}$$

if we consider that the two elements constitute a diode.

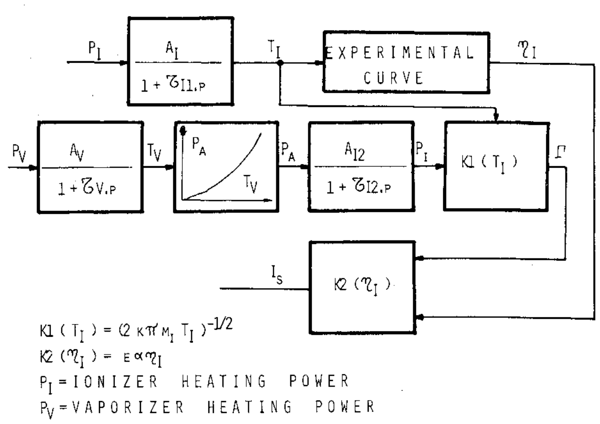

Fig. 3 Engine block diagram.

In nominal operation, the abovementioned formulas and the assumptions below: 1) beam current equal to the saturation current; 2) pressure loss small compared to the pressure upstream of the ionizer; 3) low neutralizer biasing voltage; and 4) ionization efficiency equal to 1, enable us to express the thrust vector amplitude as follows:

$$F = 5.65\ 10^8 \alpha A_i \left(\frac{eU}{k\pi}\right)^{1/2}\left(\frac{1}{T_i}\right)^{1/2} \exp(-8522/T_v)$$

Sensibility study

Thanks to the abovementioned expression we have been able to plot (Fig. 2) the relative variations of the thrust vector amplitude in function of: 1) the vaporizer temperature T_v; 2) the ionizer temperature T_i; and 3) the high voltage magnitude U.

It can be seen that the best adapted variable to control the beam current, i.e., the thrust vector magnitude, is the vaporizer temperature T_v.

Dynamic Mathematical Model

The dynamic mathematical model determination is necessary for the study of the thruster behavior around its nominal point of operation and during the start and stop sequences.

Figure 3 gives the complete block diagram illustrating the engine operation in its saturation mode. The numerical values of the time constants τ_v, τ_{i1}, and τ_{i2} and of the gains A_v and A_{i1} were obtained from experiments carried out at the "Office National d'Etudes et de Recherches Aéronautiques" (O.N.E.R.A.).

Control Loop Definition

Beam current regulation

The beam current regulation by means of the vaporizer temperature is of the proportional integral type in order to avoid a static error in the presence of perturbations that would be prejudicial to the thruster lifetime. The complete diagram of the system is shown in Fig. 4.

We shall assume that the control loop, which is electronically realized, has time constants and delays which are negligible compared to those of the direct path. After linearization, we may

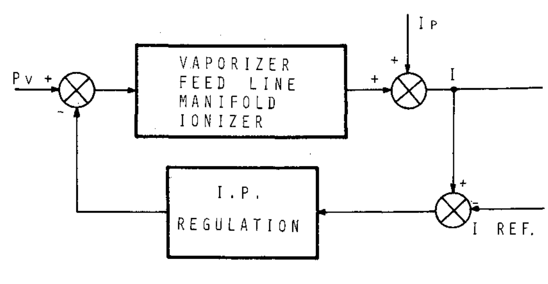

Fig. 4 General block diagram of the regulated engine.

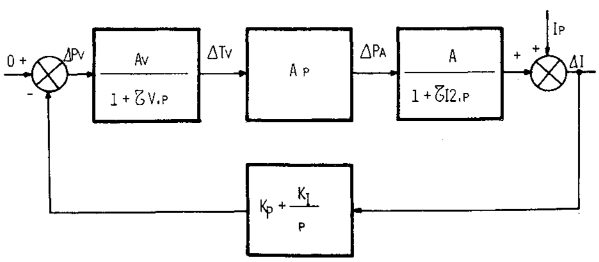

Fig. 5 Block diagram of the regulated engine after linearization.

take into account small variations only and illustrate the thruster operation around its nominal point by the diagram given in Fig. 5.[5]

The study of the system has been carried out using the root locus method with the following constraints: 1) overshoot minimization, and 2) minimum response time.

This leads to the following expressions for K_p and K_i

$$K_p = \frac{\tau_v}{4A_v A_p A\tau_{i2}} \qquad K_i = \frac{1}{4A_v A_p A\tau_{i2}}$$

Neutral flux limitation

The study we made in static and dynamic mathematical model sections does not take into account the imperfections and aging effects of the thruster, in particular those of the ionizer. Its degradation shows the necessity of a neutral flux limitation in order to keep the thruster in its nominal operating conditions. To do so, we have implemented a further regulation loop, controlled by the ionizer temperature T_i which is shown in Fig. 6.

III. Power Conditioning and Control Unit Definition

Determination of the Over-All Characteristics of the Thruster and of the Power Conditioning System

A general mission analysis together with the mathematical model that we have just described, has enabled us to implement an optimization program. The selected criteria is the total mass of the stabilization system, including the solar panel mass. The outputs of the program are the optimal thruster characteristics and the optimal thruster operating parameters. Table 1 gives the different characteristics resulting from this program for a thruster delivering a 1.5 mN thrust.

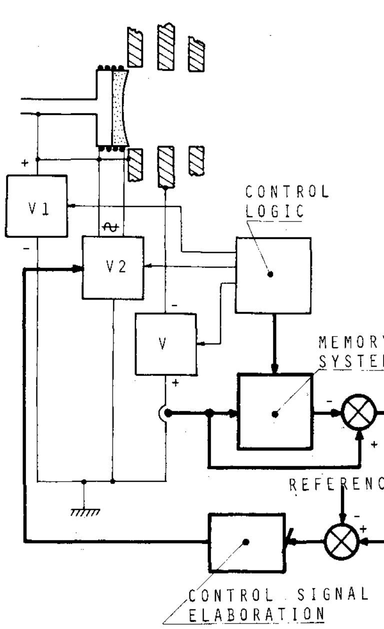

Fig. 6 Block diagram of the neutral flux limitation.

Table 1 Thruster main characteristics

Specific impulse	6700 sec
Positive high voltage	3000 v
Beam current	16.5 ma
Ionizer temperature	1473 K
Vaporizer temperature	578 K

Heating supply

All element heatings are achieved by alternating currents in order to minimize the system mass, to increase the efficiency and to obtain a zero resultant electric field (and consequently an evenly distributed emission along the neutralizer filament).

Most of the powers have been determined from the knowledge of the mathematical model. However, the current voltage characteristics are directly related to the technology used in the realization of the heating filaments.

Positive high voltage supply

The magnitude of the supply is related to the thrust vector amplitude by the following relationship:

$$F = I(2m_i U/e)^{1/2}$$

It must be able to deliver a current of 16.5 ma at 3000 v, be protected against short circuits, and be provided with a progressive turn-on device.

Negative high voltage supply

Its magnitude must be such that the total accelerating potential be sufficient to allow the thruster to operate in its saturation mode. Theoretically this supply delivers no current; practically the imperfections of the thruster generate a current which can be maintained at a value lower than 500 μa by a good system design and an efficient neutral flux regulation loop.

This supply, which is short-circuit protected, has a progressive turn-on and a regulation at 5%. This value is the result of a trade-off based on the study of the beam current to thruster total accelerating potential characteristic.

Neutralizer biasing supply

The very principle of operation of the thruster yields a delivered current equal to the beam current, i.e., 16.5 mA. The voltage which is equal to the decoupling voltage at the thruster output is a function of the neutralizer filament location. It lies

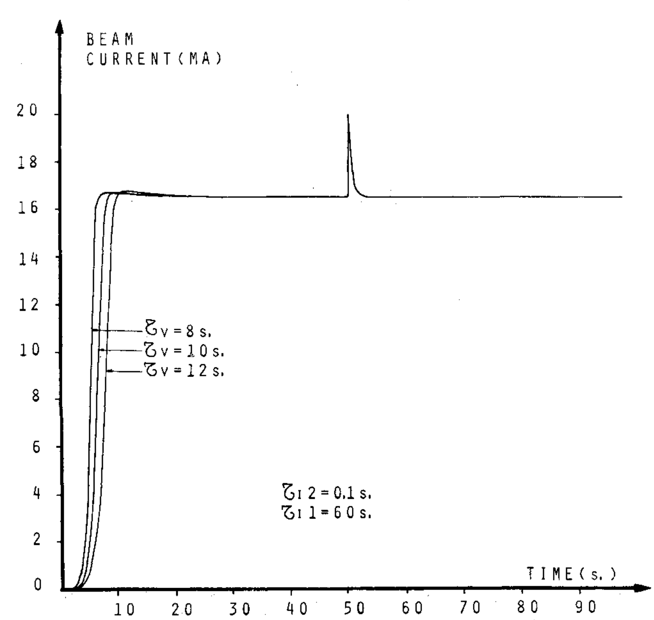

Fig. 7 Influence of ρ_v on beam current variations vs time.

Table 2 Power requirements

Power supply	Waveform	Voltage (v)	Current (mA)	Power (w)	Regulation	Short circuit protection	Insulation	Dynamic range
Ionizer polarization	d.c.	3000	16.5	49.5	+1% (v)	yes	...	0 to +3000 v
Accelerating electrode polarization	d.c.	−3000	0.5	1.5	+5% (v)	yes	...	0 to −3000 v
Neutralizer polarization	d.c.	−200	16.5	3.3	+5% (v)	yes	...	0 to −200 v
Ionizer heating	a.c.	20	1500–2000	30–40	power	yes	5 kV	...
Vaporizer heating	a.c.	3	1000	3	power	yes	5 kV	...
Valve heating	a.c.	...	...	5	power	yes	5 kV	...
Neutralizer heating	a.c.	...	...	5	+5% rms current	yes	500 v	...

in the range of 0 to −200 v and requires a voltage regulation of 5%.

Over-all characteristics

Table 2 summarizes the main characteristics of the various supplies that we briefly described in the preceding sections.

Beam current regulation loop

The aim of this section is to show the results that we have obtained with the help of a digital simulation of the thruster dynamic response. It was developed in order to study 1) the thruster turn-on phase, 2) the responses to strong beam current disturbances, and 3) the influence of the various parameter variations.

The curves shown in Fig. 7 give the beam current variations vs time in two cases: turn-on phase and beam current disturbance equal to 20% of its nominal value depict the influence of the variation of τ_v under identical conditions.

IV. Electronics Aspects

The choices that we have made concerning the different solutions possible for the PCU have been guided both in theory and experimentally by the results of the works[7–9] which have been carried out at the L.A.A.S. Also, the choices were influenced by the wish for homogenization of the different subassemblies that make up this system.

Choices Retained and Realization

Master oscillator

The master oscillator for driving the power stages is of the magnetically coupled astable variety. This choice was made, in particular, for the following reasons: 1) low power consumption, and 2) easy synchronization.

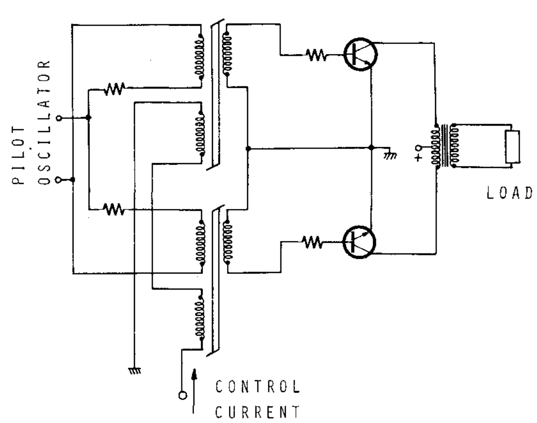

Fig. 8 Electromagnetic P.W.M. schematic diagram.

Heating power stages

The search for homogenization and the need for alternating heating currents led us to choose push-pull power stages.

The control of the different invertors is achieved by pulse width modulation obtained by an electromagnetic method rather than an electronic method due to the low number of active components and the relative ease with which it is implemented. The diagram of the principle of this device and the power stage is given in Fig. 8.

Positive high voltage supply

The output voltage must be variable from 0 to +3kv and hence we have chosen a "buck-boost" switching regulator. This enables a high efficiency to be obtained together with a minimization of the size and mass of the output transformer.

Negative high voltage supply

This power supply consists of a push-pull power stage followed by a symmetric voltage multiplier.[10] The latter is of interest when the size and mass of the transformer are limited by the number of secondary turns rather than the output power.

Beam current regulation loop

Figure 9 gives the block diagram of the regulation loop. The measurement of the beam current is compared with a reference that fixes the nominal value. The error signal obtained is passed through a power limiting system and put into a suitable form so as to supply the control voltage of the vaporizer heating invertor.

Realization of an Operational Prototype: Principal Characteristics

The operational prototype that has been realized presents the following characteristics. 1) Modular construction so as to facilitate tests and maintenance, each module constitutes a subsystem of the PCU. 2) Use of components having space approved equivalents. 3) Numerous possibilities of adjustment, especially concerning the powers delivered, enabling simple adaptation.

So as to verify the operation and to measure the performances of these modules, they have been connected onto dummy loads that simulate the different thruster subsystems in the steady state.

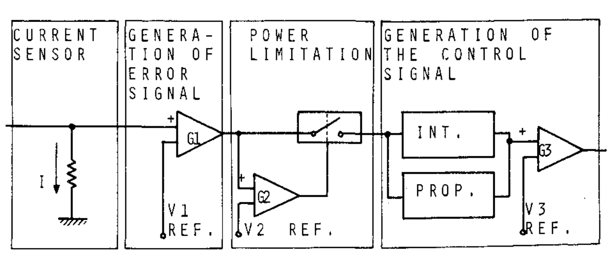

Fig. 9 Beam current regulation loop block diagram.

Efficiencies

The different efficiencies obtained are summarized in Table 3. The over-all efficiency (power supplies, regulation loop, sequential system, etc.) is in the order of 85%.

Table 3 Power supplies efficiencies

	Efficiency (%)
Positive high voltage supply	89
Negative high voltage supply	60
Neutralizer polarization supply	78
Ionizer heating supply	94
Vaporizer heating supply and beam current regulation loop	80
Valve heating supply	90
Neutralizer filament heating supply	84

Reliability

The reliability figure R has been calculated for an application to a 400 Kg satellite and a mission of 5 yr, the total thrust time being 5000 hr and the component failure probabilities being divided by ten during the stop phases. The results obtained are given in Table 4.

Table 4 PCU reliability

Normal fabrication		Fabrication with reliability program	
Laboratory	Satellite in orbit	Laboratory	Satellite in orbit
0.5117	0.2475	0.9217	0.8856

V. Test Results

In this paragraph, we shall briefly describe the results of the trials of the PCU that have been carried out on a monobutton thruster at the ONERA[11] with the double aim of: 1) verifying the correct operation of the power supplies during all the operational phases of the thruster; and 2) verifying the principle by which the beam current is regulated and of the corresponding subsystem.

Trials of the High Voltage Power Supplies

The first trial was carried out after the thruster had been thoroughly cleaned and consequently the start up resulted in very few internal flashovers. For the second trial, the thruster was restarted without cleaning and consequently there was a certain internal pollution, an increase of the initial accelerating electrode current and a decrease of the latter with time as the cesium was evacuated.

Trials of the Regulation Loops

Figure 10 shows a stable regime without regulation, the variation of the currents between marks 18.5 and 21 were provoked by variations in the reservoir heating. Figure 11 shows the collector current taken as an information parameter, the regulation loop being in operation.

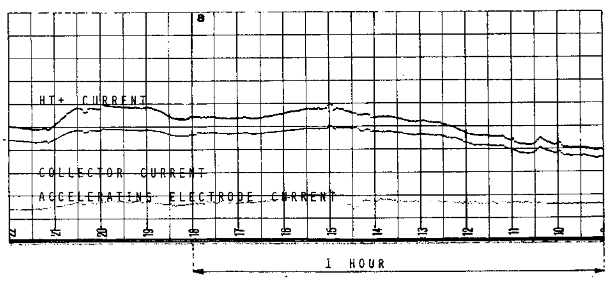

Fig. 10 Engine currents variations vs time without regulation.

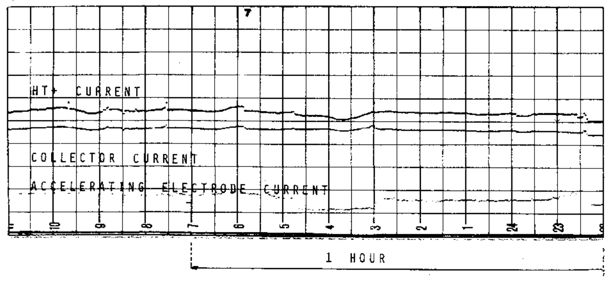

Fig. 11 Engine currents variations vs time with regulation.

One notes that the collector current is nearly constant despite the numerous perturbations due to variations of: the ionizer heating bombardment current, the reservoir heating, and the cesium flow rate.

Conclusion

The main conclusions that can be drawn from such a study are of two types.

1) Knowledge of a mathematical model (static and dynamic) based both on the theoretical relationships and the experimental results enables the definition and implementation of the regulation systems that are necessary for normal operation and for the dynamic thruster sequences. The regulation systems enable optimal thruster utilization throughout the mission, the quality criteria being the faithful operation and the lifetime.

2) The design and realization of the thruster associated electronics can only be efficiently carried out in close collaboration with the thruster technology specialists on one hand and the system parameter measurement specialists on the other hand.

References

[1] Mutin, J., "The Objectives of the C.N.E.S. in the Field of Electric Propulsion," paper presented at the Conference on Electric Propulsion of Space Vehicles, April 10–12, 1973, Abingdon, Berks., England.

[2] Landrault, C., "Le Propulseur à Ionisation de Césium par Contact. Optimisation par la Mise au Point du Modèle Mathématique. Conception et Réalisation des Systèmes de Conditionnement de Puissance et de Commande," Thèse de Docteur-Ingénieur, No. 379, May 15, 1973, Université Paul Sabatier, Toulouse, France.

[3] Briot, M., Landrault, C., and Marrot, C., "General Ideas on Power Conditioning and Control of Electric Propulsion: Application at the Case of Ion Cesium Contact Thruster," paper presented at the Conference on Electric Propulsion of Space Vehicles, April 10–12, 1973, Abingdon, Berks., England.

[4] Brewer, G. R., *Ion Propulsion: Technology and Applications*, Gordon and Breach, New York, 1972.

[5] Dorf, R. C., *Modern Control Systems*, Addison-Wesley, Reading, Mass., 1970.

[6] Lagasse, J., Costes, A., and Laprie, J. C., "Synthesis of the Studies Carried Out by the 'Laboratoire d'Automatique et de ses Applications Spatiales du C.N.R.S.' on the Satellite Stabilization by Ion Thrusters," AIAA Paper 72-437, Bethesda, Md., 1972.

[7] Durante, C., "Contribution à L'Étude des Circuits Statomagnétiques en Régime de Commutation," Thèse de Doctorat ès Sciences, 205, June 20, 1963, Université Paul Sabatier, Toulouse, France.

[8] Cammas, H., Marpinard, J. C., Prajoux, R., and Quemener, Y., "Commande d'un Transistor Interrupteur par Transformateur d'Intensité," paper presented at the Journées d'Etudes sur la Propulsion Electrique dans ses Applications Spatiales," June 21–23, 1972, Toulouse, France.

[9] Briot, M., "Contribution à L'Étude des Convertisseurs Continu-Continu. Réalisation d'un Convertisseur à Tension de Sortie Variable Commandable," Thèse de Doctorat de Spécialité, No. 1038, Dec. 22, 1970, Université Paul Sabatier, Toulouse, France.

[10] Powell, D. R., "Rapport de Stage de D.E.A.," June 20, 1973, L.A.A.S., Toulouse, France.

[11] Briot, M. and Labbe, J., "Essais du Sous-Ensemble de Conditionnement de Puissance Effectués sur un Propulseur Monobouton à l'ONERA," Note Technique TNPE 73 T 17, June 1973, L.A.A.S., Toulouse, France.